RESEARCH

Carvacrol induces osteogenic differentiation of BMSCs and alleviates osteolysis in aged mice by upregulating lncRNA NEAT1 to promote SIRT1 expression

Zefeng Xu[a], Zeyu Wang[a], Wenming Ma[a], Zhihui Huang[a,*]

[a] *Department of Traumatic Orthopedics, The First People's Hospital of Changzhou, the Third Affiliated Hospital of Soochow University, Changzhou, Jiangsu Province, China.*

Abstract

Background: Wear particle-induced periprosthetic osteolysis is a major contributor to joint replacement failure and revision surgery in the elderly. Osteogenic differentiation of bone marrow-derived mesenchymal stem cells (BMSCs) is a promising approach for bone regeneration. Carvacrol may have bone-protective potential. This study investigated whether carvacrol alleviates osteolysis and promotes osteogenic differentiation of BMSCs by regulating SIRT1 expression.

Materials and Methods: An osteolysis model in aged mice was established by titanium (Ti) particle induction. BMSCs were isolated from femur and tibia of 18-month-old mice and cultured in osteogenic differentiation medium. RIP and RNA pull-down were used to evaluate the binding of SIRT1 and lncRNA NEAT1. Ubiquitination analysis was performed to investigate NEAT1-mediated regulation of SIRT1 ubiquitination modification levels.

Results: Carvacrol treatment improved Ti particle-induced calvarial erosion and attenuated osteolysis. Carvacrol increased SIRT1 both in the mouse model of Ti-induced osteolysis and in BMSCs under osteogenic differentiation. Carvacrol treatment promoted ALP activity, bone mineralization capacity, and expression of osteogenic differentiation-related factors, whereas SIRT1 knockdown reversed this effect. LncRNA NEAT1 interacted with SIRT1, and overexpression of NEAT1 stabilized SIRT1 by inhibiting its ubiquitination modification. NEAT1 knockdown altered the promoting effect of carvacrol on osteogenic differentiation of BMSCs, while overexpression of SIRT1 reversed the effects of NEAT1 knockdown. Similarly, NEAT1 knockdown altered the inhibitory effect of carvacrol on osteolysis *in vivo.*

Conclusion: Our research results demonstrate that carvacrol showed potential in treating osteolysis in aged mice by regulating NEAT1 to promote the expression of SIRT1 and can facilitate the osteogenic differentiation of BMSCs.

Keywords: Osteolysis, carvacrol, bone marrow-derived mesenchymal stem cells, NEAT1, SIRT1

Introduction

Total hip arthroplasty (THA), total knee arthroplasty (TKA), and total joint arthroplasty (TJA) are among the most common orthopedic surgeries used to treat severe joint injuries, rheumatoid arthritis, osteoarthritis, and other

end-stage joint diseases [1]. TKA surgery is typically performed in elderly patients with conditions such as rheumatoid arthritis [2], while TJA is a common and effective surgery for older patients (>65 years) with late-stage osteoarthritis [3, 4]. Despite the maturity of these surgeries, some patients still require further surgical revision, mainly due to aseptic loosening [5]. The main cause of aseptic loosening is the accumulation of wear particles around the implant, such as titanium (Ti) particles [6]. Wear particles are reported to induce osteolysis by disrupting the differentiation, survival, and function of osteoblasts and osteoclasts, resulting in an imbalance between bone formation and resorption [7-10]. Bone marrow-derived mesenchymal stem cells (BMSCs) are important for bone regeneration due to their multipotent differentiation ability, as they can differentiate into various cell types, including osteoblasts,

chondrocytes, and adipocytes, thereby aiding in bone tissue regeneration and repair [11-14]. In addition, BMSCs secrete growth factors and extracellular matrix molecules that promote angiogenesis, cell proliferation, and differentiation [15]. Therefore, it is important to study the differentiation mechanism of BMSCs to promote osteoblast differentiation and alleviate osteolysis around prostheses. Carvacrol (2-methyl-5-[1-methylethyl] phenol) is a volatile oil component found primarily in herbaceous plants such as oregano, peppermint, and thyme [16]. It has anti-inflammatory, antioxidant, and antimicrobial properties [17, 18]. Research suggests that carvacrol can effectively reduce tissue damage and bone loss associated with ligature-induced periodontitis [19, 20]. Deepak *et al*. discovered that carvacrol inhibits osteoclastogenesis and negatively regulates the survival of mature osteoclasts [18]. In addition, carvacrol has a bacteriostatic effect on osteoblast proliferation without cytotoxic effects [21]. Based on the existing literature, we speculate that carvacrol may have a therapeutic effect in osteolysis. There is evidence that carvacrol is involved in the differentiation of mesenchymal stem cells. Specifically, it has been observed that carvacrol can reduce the differentiation of mesenchymal stem cells derived from umbilical cord tissue into adipocytes [22]. Furthermore, at low concentrations, carvacrol can promote the paracrine potential and endothelial differentiation of bone marrow mesenchymal stem cells in angiogenesis [23]. Therefore, we speculate that carvacrol induces osteogenic differentiation of BMSCs to alleviate osteolysis.

Numerous studies have demonstrated that silent information regulator type 1 (SIRT1) has a therapeutic effect on osteolysis [24-27]. Studies have shown that promoting osteogenic potential in BMSCs through SIRT1 can improve osteolysis [27]. Upregulation of SIRT1 was found to promote osteogenic differentiation in BMSCs [28, 29]. Runx2 and Osterix, which are the primary transcription factors involved in osteogenesis [30], are positively regulated by SIRT1. In addition, the expression of osteogenesis-related factors, including osteocalcin (OCN), osteopontin (OPN), and sialoprotein, is reduced in SIRT1 knockout cells [31-33]. Although research has shown that carvacrol upregulates SIRT1 levels [34], the specific regulatory mechanism is not yet understood.

Long non-coding RNAs (lncRNAs), as a type of non-coding RNA, have been recognized as key regulatory molecules involved in gene expression, epigenetic modifications, and protein activity [35]. Recently, lncRNAs have been found to be involved in the process of osteolysis. For example, lncRNA TSIX has been shown to promote osteoblast apoptosis in particle-induced osteolysis [36]. LncRNA DANCR contributes to osteolysis by inhibiting osteoblast differentiation [37]. Similarly, LncRNA KCNQ1OT1 improves particle-induced osteolysis by inducing macrophage polarization [38]. NEAT1 and XIST promote osteogenic differentiation of human bone marrow mesenchymal stem cells [39, 40], but there is no clear literature reporting their involvement in osteolysis.

Therefore, this study proposes to use a mouse model of osteolysis and Ti particle-induced BMSCs to investigate the potential therapeutic effects of carvacrol on osteolysis in aged mice. In addition, this study will investigate whether carvacrol induces the expression of SIRT1 through the mediation of NEAT1 to promote the osteogenic differentiation of BMSCs. The results of this study promise to provide new ideas and methods for the treatment of osteolysis.

Materials and Methods

Ti particle-induced osteolysis model

As previously described, a mouse model of osteolysis was established to determine the protective effect of carvacrol on osteolysis in aged mice [41]. SPF grade C57BL/6 mice (18 months old) were obtained from Changzhou Cavens Laboratory Animal Co., Ltd. The living conditions of the mice were as described previously [42]. The mice were housed in a controlled environment with a temperature of 22-24°C and humidity of 50%. Prior to the start of the experiment, the mice underwent a 1-week period of ad libitum feeding and acclimatization.

Mice were anesthetized by intraperitoneal injection of ketamine and xylazine. After anesthesia, the skin at the calvarial area was gently scraped and disinfected with 10% povidone-iodine solution, and then cut along the midline with a sharp scalpel. Then, 30 mg titanium particles (30 μL) were evenly distributed on the surface of the bilateral parietal bones, and the surgical skin incision was closed. In the sham + PBS group, an equivalent volume of PBS (30 μL) was used instead of the titanium particle suspension. After establishment of the model, carvacrol (5 or 10 mg/kg) was administered intragastrically daily for 2 weeks, while PBS was administered daily to mice in the sham + PBS and Ti + PBS groups. For the Ti + Carvacrol + LV-shRNA and Ti + Carvacrol + LV-sh-NEAT1 groups, 70 μL of LV-sh-NEAT1 or LV-shRNA (titer: 8×10^8 TU/mL) was injected locally into the calvarial area immediately after completion of surgery. The injection site was determined to be 2 mm from the midline and on the right lateral side of the surgical incision. Upon completion of the injection, the mice were administered carvacrol at a dose of 10 mg/kg. To euthanize the mice, an intraperitoneal injection of 480 mg/kg Avertin was administered. Calvarial bones were dissected and fixed in 4% paraformaldehyde for 2 days. After fixation, calvarial samples were washed three times with PBS and then stored in 75% ethanol at 4°C until further analysis.

Micro-computed tomography (Micro-CT) scan

Carefully remove Ti particles from each calvaria to avoid metal artifacts in the scan results. Then, fix the harvested mouse calvaria and use a micro-CT scanner (Skyscan 1272, Bruker, Germany). Set the scan resolution to 9 μm and the X-ray energy to 50 kV and 500 μA. Initiate the scanning process by rotating the scanning stage and exposing the specimens to the X-ray beam, taking a series of projection images of the calvarial region. Use the

software provided by the manufacturer to perform three-dimensional image reconstruction. Following the methods established in previous studies [43], use the micro-CT analysis software (Skyscan) to evaluate different tissue morphometric measurements: bone density (g/cm^3) and bone volume/total volume (BV/TV, %).

Cell culture of BMSCs and osteogenic differentiation

BMSCs were cultured and differentiated as previously described [44]. Briefly, BMSCs were isolated from the femur and tibia of 18-month-old C57BL/6 mice. Cells were cultured in MEM alpha medium (α-MEM, 11900024, Gibco, USA) supplemented with 2 mM glutamine, 20% fetal bovine serum (FBS, 12483020, Gibco, USA), 100 U/mL penicillin, and 100 μg/mL streptomycin (15140122, Invitrogen, USA). Cells were maintained in a cell culture incubator at 37°C with 5% carbon dioxide. BMSCs were seeded in 12-well plates at a density of 1×10^5 cells per well. When the cell density reached approximately 70-80%, osteogenic induction differentiation was initiated. For osteogenic differentiation, cells were incubated in Dulbecco's modified Eagle's medium (DMEM) supplemented with 10% FBS, 10% horse serum, 12 mM L-glutamine, 20 mM β-glycerol phosphate, 100 μg/mL streptomycin, 50 ng/mL thyroxine, 1 nM dexamethasone, 100 U/mL penicillin, and 0.5 μM ascorbate 2-phosphate. For Ti and carvacrol treatments, Ti (1.0 mg/mL) or carvacrol (12.5, 25, and 50 μM) was added simultaneously at the start of osteogenic induction.

Lentivirus infection

NEAT1 overexpression lentiviruses (LV-NEAT1), SIRT1 overexpression lentiviruses (LV-SIRT1), negative control (LV-NC), NEAT1 RNA interference lentiviruses (LV-sh-NEAT1), and negative control (LV-shRNA) were purchased from GenePharma (China). The lentiviral suspensions containing polybrene (5 mg/mL) were added to the cell proliferation medium. After 48 hours of incubation, cells were selected with puromycin (1 μg/mL).

Alkaline phosphatase (ALP) activity

After 7 days of cultivation in osteogenic differentiation medium, BMSCs were subjected to ALP activity assessment using an ALP detection kit (P0321S, Beyotime, China). Cells were lysed using RIPA lysis buffer (P0013B, Beyotime, China), and the appropriate reagents were added according to the manufacturer's instructions. The mixture was incubated at 37°C for 10 minutes. After the reaction was stopped, the absorbance was measured at 405 nm to quantify the ALP activity in the samples.

Alizarin red S (ARS) staining

The mineralization ability of the cells was evaluated using an ARS staining kit (C0148S, Beyotime, China). After 21 days of induction and differentiation, the culture medium was removed and the cells were washed once with PBS. The cells were then fixed with a fixative solution for 20 minutes, followed by three washes with PBS. Next, 0.5% ARS working solution was added to detect calcium deposits according to the kit instructions. The samples were examined under a light microscope (Leica, Germany).

Western blot analysis

The experimental procedure for protein extraction from cryopreserved calvarial tissue samples was as follows: samples were washed 2-3 times with prechilled PBS. A mixture of 2% protease phosphatase inhibitor and 200 μL RIPA protein lysis buffer was then added to the samples, followed by thorough grinding. After sufficient grinding, 300 μL protein lysis buffer was added and mixed evenly. For BMSCs, lysis was performed on ice using RIPA protein lysis buffer containing phenylmethanesulfonyl fluoride (PMSF, 100 mM). After lysis was completed, the supernatant was collected by centrifugation. Then, 2 μL of the protein solution was collected for protein concentration measurement using a BCA assay kit (P0012, Beyotime, China). Next, the protein samples were separated by SDS-polyacrylamide gel electrophoresis. The separated proteins were then transferred to a polyvinylidene fluoride membrane (PVDF, 88518, ThermoFisher Scientific, USA). The membrane was blocked with 5% skim milk for one hour at room temperature. Specific primary antibodies were added and incubated with the PVDF membrane overnight at 4°C: anti-SIRT1 (ab263965, Abcam, USA), anti-RUNX2 (ab114133, Abcam, USA), anti-Osterix (ab209484, Abcam, USA), anti-OCN (ab93876, Abcam, USA), anti-OPN (ab8448, Abcam, USA), and anti-β-actin (ab8227, Abcam, USA). After three washes with Tris-HCl buffer saline and Tween (TBST), the membrane was incubated with the corresponding secondary antibody (HRP-conjugated anti-mouse IgG or anti-rabbit IgG) for 1 hour. Specific protein signals were detected using a chemiluminescence assay (PE0010, Solarbio, China). Images were captured using an Amersham Imager 600 system (GE Healthcare, USA).

Reverse transcription-quantitative PCR (RT-qPCR)

After culturing BMSCs in osteogenic induction medium for seven days, Trizol reagent (15596026, ThermoFisher Scientific, USA) was added to completely lyse the cells for RNA extraction. After the RNA concentration was detected by spectrophotometer, the extracted total RNA was used as a template, and the reverse transcription reaction was performed according to the instructions of the M-MLV Reverse Transcription Kit manual (M1701, Promega, USA). The PCR reaction system was constructed according to the Fast SYBR Mixture reaction kit (CW0955M, CWBIO, China). Finally, qPCR was performed using the ABI 7000 real-time fluorescence quantitative PCR system (Applied Biosystems, USA). Relative gene expression levels were calculated using the $2^{-\Delta\Delta Ct}$ formula.

RNA pull-down

RNA probes were synthesized by GenePharma and labeled with biotin (Bio-NEAT1 or Bio-NC). The experiment was performed according to the instructions of the RNA-Protein Pull-Down Assay Kit (20164, ThermoFisher Scientific, USA). Briefly, BMSCs were lysed with lysis

buffer, and then the synthesized RNA probes were incubated with the lysate at room temperature for 30 minutes. The biotinylated RNA probe specifically binds to streptavidin-coated magnetic beads to form an RNA probe-bead complex. Wash buffer is used several times to remove non-specifically bound proteins and RNA molecules. The specific binding proteins are eluted from the RNA probe-bead complex and the RNA-protein complex is detected by Western blotting.

RNA immunoprecipitation (RIP)

RIP experiments were performed using the EZ-Magna RIP Kit (17-701, Millipore, USA) to verify the binding between SIRT1 and NEAT1. The cross-linked cells were completely lysed with RIPA lysis buffer. SIRT1 antibody and magnetic beads were then added to the lysed samples for immunoprecipitation. Non-specifically bound proteins and impurities were removed by multiple washing steps. Finally, RNA was extracted from the immunoprecipitated samples and the RNA samples were analyzed by RT-qPCR.

Ubiquitination assay

BMSCs were transfected with HA-ubiquitin (Ub) and LV-NEAT1 (or LV-NC). After 24 hours of transfection, MG132 (10 μM) was added to the medium and the cells were incubated for 4 hours. The cells were washed twice with PBS and lysed with RIPA lysis buffer. After centrifugation, the supernatant was transferred to a new EP tube and 50 μL beads were added to the supernatant. The cell lysate was incubated with anti-SIRT1 antibody at 4℃ overnight for immunoprecipitation. Wash solution (500 μL sterile PBS buffer + 50 μL protease inhibitor) was prepared. Centrifuge at 7500 rpm for 5 min and discard the supernatant. Wash solution is added to the tube, quickly mixed and centrifuged. Discard the supernatant, leaving the beads in each tube. 50 μL of 6 × loading buffer was added to each tube, vortexed to mix thoroughly, and boiled in a 100℃-metal bath for 10 min. Immunoblotting (IB) was then performed to detect binding proteins using anti-HA (ab137838, Abcam, USA) and anti-SIRT1.

Immunoprecipitation (IP) and IB assay

BMSCs were transfected with LV-NEAT1 (or LV-NC). After 24 h of transfection, MG132 (10 μM) was added to the medium and the cells were incubated for 4 hours. Cells were lysed with RIPA lysis buffer containing PMSF. The supernatant of the lysed cells was mixed with protein A/G agarose, and the centrifuge tube was gently shaken at 4℃. Anti-SMURF2 (ab313470, Abcam, USA) was then added and incubated overnight at 4℃. Finally, the target protein and its interacting proteins were eluted with elution buffer. Immunoblotting and detection of eluted proteins were performed using anti-SIRT1 and anti-SMURF2.

Statistical analysis

All data analysis was performed using GraphPad Prism 6.0. All numerical values are presented as mean ± standard deviation (SD). Two-tailed unpaired Student's t-test was used to compare mean differences between two independent samples. Comparison between groups was performed using one-way ANOVA followed by Tukey's multiple comparison test or two-way ANOVA followed by Bonferroni's multiple comparison test. A P value < 0.05 was considered statistically significant.

Results

Carvacrol alleviates osteolysis in aged mice *in vivo*

To investigate the role of carvacrol in osteolysis, we examined the calvarial condition of elderly mice in a mouse model of osteolysis induced by Ti particles treated with different doses of carvacrol. We evaluated the calvarial conditions of different groups using micro-CT scanning. Three-dimensional reconstructed images showed that, compared with the sham + PBS group, the calvarial bone of the Ti + PBS group was extensively eroded and the calvarial thickness was reduced. However, carvacrol treatment significantly improved the calvarial erosion (Figure 1A). Further analysis revealed that the Ti + PBS group had a significant reduction in bone density and BV/TV compared to the sham + PBS group (Figure 1B-C). Interestingly, treatment with 5 or 10 mg/kg carvacrol significantly increased the bone density reduction induced by Ti particles (Figure 1B), and only 10 mg/kg carvacrol treatment significantly upregulated the BV/TV level (Figure 1C). Taken together, these results indicate that carvacrol has a protective effect against Ti particle-induced osteolysis.

To further elucidate the role of carvacrol in osteoblast differentiation, we examined the expression levels of SIRT1 and osteoblast differentiation-related factors (RUNX2, Osterix, OCN, and OPN) in the calvaria of aged mice. Western blot analysis revealed that the expression of SIRT1, RUNX2, Osterix, OCN, and OPN was significantly decreased after Ti treatment, while carvacrol treatment effectively reversed this phenomenon (Figure 1D). These results suggest that carvacrol has the potential to promote osteoblast differentiation.

Carvacrol alleviates osteogenic differentiation of Ti-inhibited BMSCs *in vitro*

To determine the appropriate concentration of carvacrol to promote the differentiation of BMSCs into osteoblasts, we performed ARS staining and ALP activity analysis on different concentrations of carvacrol-treated groups and control groups. The results showed that the mineralization ability of BMSCs was significantly enhanced when the concentration of carvacrol exceeded 25 μM (Figure S1A). When the concentration of carvacrol exceeded 12.5 μM, the ALP activity of BMSCs was observed to be promoted (Figure S1B). At the same time, we evaluated the expression of osteogenic differentiation-related factors and found that the expression of RUNX2 and OCN in BMSCs was promoted when the concentration of carvacrol exceeded 25 μM (Figure S1C&E). In addition, the expression of Osterix and OPN in BMSCs was also promoted when
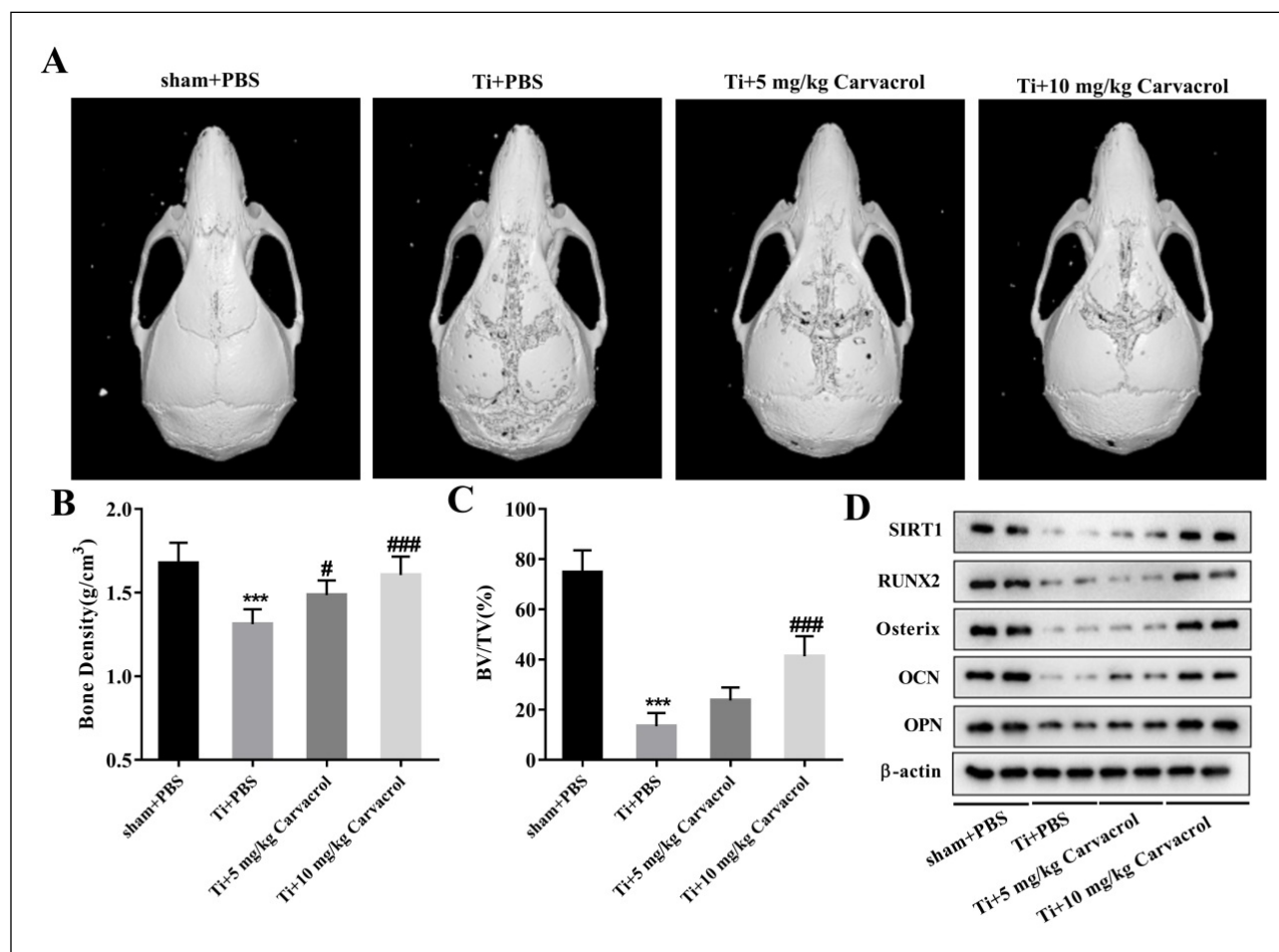
Figure 1. Carvacrol attenuates osteolysis in elderly mice *in vivo*. After establishing the osteolysis model with Ti particles, carvacrol (5 mg/kg or 10 mg/kg) was administered daily for two weeks. The sham + PBS and Ti + PBS groups received the same amount of PBS. (A) Representative micro-CT three-dimensional reconstructed images of mouse calvaria in each group. (B-C) Bone density (g/cm3) and BV/TV (%) of each group were measured. All values are expressed as mean ± SD. One-way ANOVA was performed by Tukey's multiple comparison test, and statistically significant differences are indicated by: ***$P < 0.001$ *vs*. Sham + PBS group; #$P < 0.05$, ###$P < 0.001$ *vs*. Ti + PBS group. (D) The expressions of PSIRT1, RUNX2, Osterix, OCN, OPN, and β-actin in each group were detected by Western blotting. β-Actin was used as an internal control for equal amounts of protein applied.

the concentration of carvacrol exceeded 12.5 μM (Figure S1D&F). Based on these results, we concluded that carvacrol at a concentration of 25 μM significantly promoted osteogenic differentiation. Therefore, we chose this concentration for the following experiments.

To further investigate whether the protective effect of carvacrol against osteolysis occurs by promoting osteogenic differentiation of BMSCs, we first measured the expression of osteogenic differentiation-related factors. The results showed that carvacrol treatment significantly promoted the expression of RUNX2, Osterix, OCN, and OPN in Ti-inhibited mouse BMSCs (Figure 2A-D). To further elucidate the role of carvacrol in the function of BMSCs, we next examined ALP activity. Ti inhibited the ALP activity of BMSCs, whereas carvacrol treatment reversed this result (Figure 2E). To evaluate whether carvacrol promotes the mineralization capacity of BMSCs, we performed ARS staining. Ti significantly reduced the osteogenic capacity of BMSCs, whereas carvacrol reversed these effects (Figure 2F). Taken together, these observations suggest that carvacrol effectively alleviates the Ti-inhibited osteogenic differentiation of BMSCs. Furthermore, compared with the control group, the expression of SIRT1 was significantly decreased in the Ti group, whereas the addition of carvacrol treatment significantly upregulated the expression level of SIRT1, which is consistent with the results in mice (Figure 2G). Therefore, we speculate that carvacrol may induce osteogenic differentiation of BMSCs and alleviate osteolysis by upregulating the expression of osteogenic differentiation-related factors and SIRT1. However, further validation is needed to confirm this hypothesis.

Carvacrol alleviates osteogenic differentiation of Ti-inhibited BMSCs by upregulating SIRT1

To further confirm the regulatory role of carvacrol on SIRT1 during osteogenic differentiation of BMSCs, we transfected BMSCs with LV-sh-SIRT1 or LV-shRNA (negative control). Compared with the Ti + Carvacrol + LV-shRNA group, the significant decrease of SIRT1 expression in BMSCs transfected with LV-sh-SIRT1 indicates the efficacy of transfection (Figure 3A). Carvacrol treatment significantly upregulated the expression of osteoblast differentiation-related factors (RUNX2, Osterix,
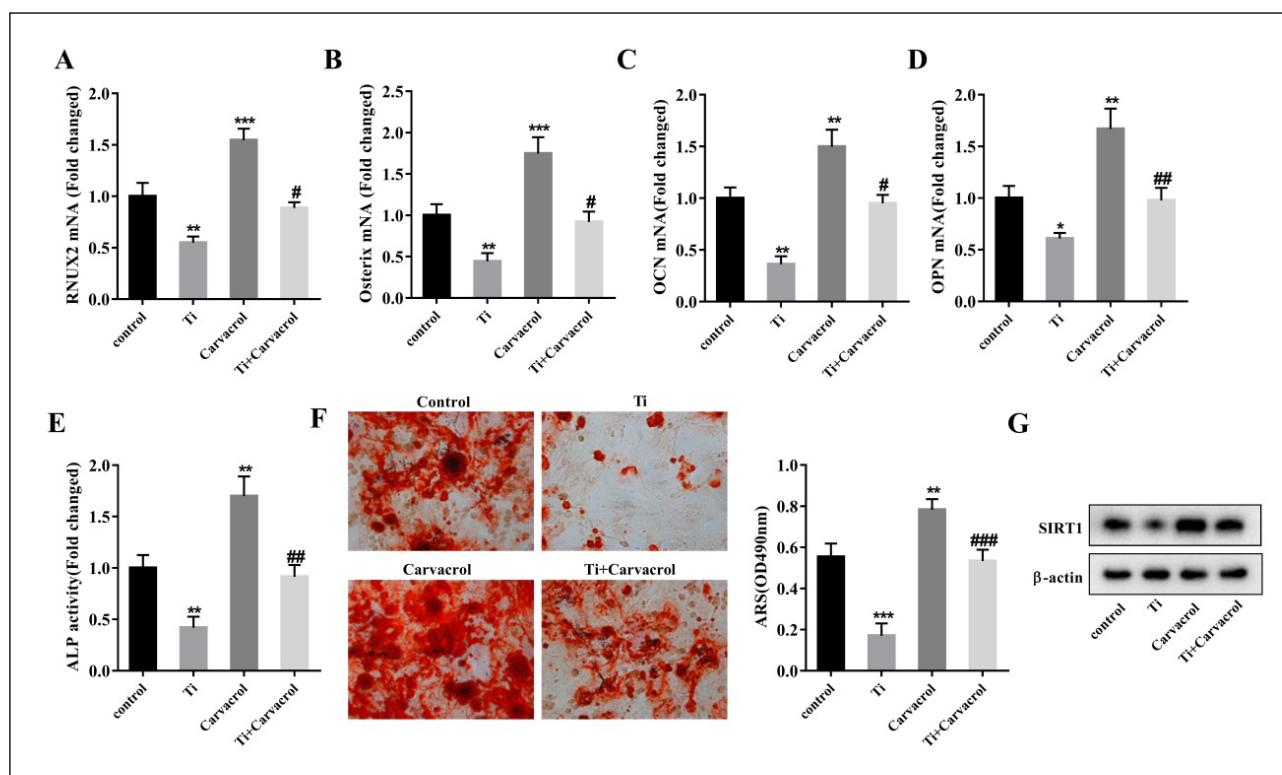
Figure 2. Carvacrol attenuates osteogenic differentiation of Ti-inhibited BMSCs *in vitro*. BMSCs were stimulated with Ti particles and treated with carvacrol at a concentration of 25 μM. RT-qPCR analysis of relative mRNA levels of osteoblast differentiation-related factors, including RUNX2 (**A**), Osterix (**B**), OCN (**C**), and OPN (**D**), in the supernatant of BMSCs from each group. (**E**) Quantitative analysis of ALP activity of BMSCs. (**F**) After carvacrol treatment, BMSCs were cultured in osteogenic induction medium and stained with ARS on day 21. Representative images of ARS staining. Mineralized nodules were quantified by calculating the ratio of mineralized area to total area after staining. One-way ANOVA was performed using Tukey's multiple comparison test, and statistically significant differences are indicated by: *$P < 0.05$, **$P < 0.01$, ***$P < 0.001$ *vs*. control group; #$P < 0.05$, ##$P < 0.01$, ###$P < 0.001$ *vs*. Ti group. (**G**) The relative protein expression levels of SIRT1 in each group of BMSCs were evaluated.

OCN, OPN), and LV-sh-SIRT1 partially reversed the effect of carvacrol (Figure 3B-E). Further analysis of the osteogenic potential of BMSCs revealed that carvacrol promoted ALP activity and mineralization ability, which was partially reversed by LV-sh-SIRT1 (Figure 3F-G). Collectively, these results suggest that carvacrol alleviates titanium inhibition of osteogenic differentiation in BMSCs by upregulating SIRT1.

Carvacrol promotes SIRT1 expression through NEAT1

To further investigate the promoting effect of carvacrol on SIRT1 expression, we used software prediction and combined with existing literature to identify potential lncRNAs that may interact with SIRT1 and play a role in osteolysis or osteoblast differentiation processes. The selected lncRNAs are as follows: TSIX [36], DANCR [37], KCNQ1OT1 [38], NEAT1 [39], and XIST [40]. Therefore, we cultured BMSCs under the treatment of carvacrol at a concentration of 25 μM and evaluated the expression levels of lncRNAs by RT-qPCR after 48 hours of incubation. The results showed a significant upregulation of NEAT1 expression in response to carvacrol (Figure 4A). Therefore, we hypothesize that carvacrol may affect SIRT1 by regulating NEAT1.

To determine the interaction between NEAT1 and SIRT1, we performed an RNA pull-down assay using biotin-labeled lncRNA-NEAT1 (Bio-NEAT1) and detected SIRT1 in the pulled-down complexes by Western blotting. The results showed that SIRT1 was enriched in the Bio-NEAT1 pulled-down complexes compared to the Bio-NC (Figure 4B). In addition, we performed a RIP assay using specific antibodies to precipitate SIRT1, followed by RT-qPCR to determine the levels of NEAT1 in the precipitated material. The results showed a significant enrichment of NEAT1 in the immunoprecipitated complex of SIRT1 (Figure 4C). Furthermore, we used LV-sh-NEAT1 plasmids to transfect BMSCs. Remarkably, the downregulation of NEAT1 resulted in a significant decrease in the expression level of SIRT1 (Figure 4D), providing further evidence for the interaction between NEAT1 and SIRT1.

We then investigated whether carvacrol affects SIRT1 expression through NEAT1. BMSCs were divided into the following groups: control, Ti, Ti + carvacrol, Ti + carvacrol + LV-shRNA, and Ti + carvacrol + LV-sh-NEAT1. Western blot analysis revealed that carvacrol significantly promoted the expression of SIRT1 protein, but this promotion was altered in the presence of LV-sh-NEAT1 (Figure 4E). In addition, RT-qPCR analysis of the calvarial samples in Figure 1 showed that NEAT1 expression was significantly downregulated in the Ti + PBS group compared with the sham + PBS group. However, the introduction of carvacrol resulted in the upregulation of NEAT1 levels (Figure 4F). The data presented strongly support the notion that NEAT1 plays a critical role in facilitating the
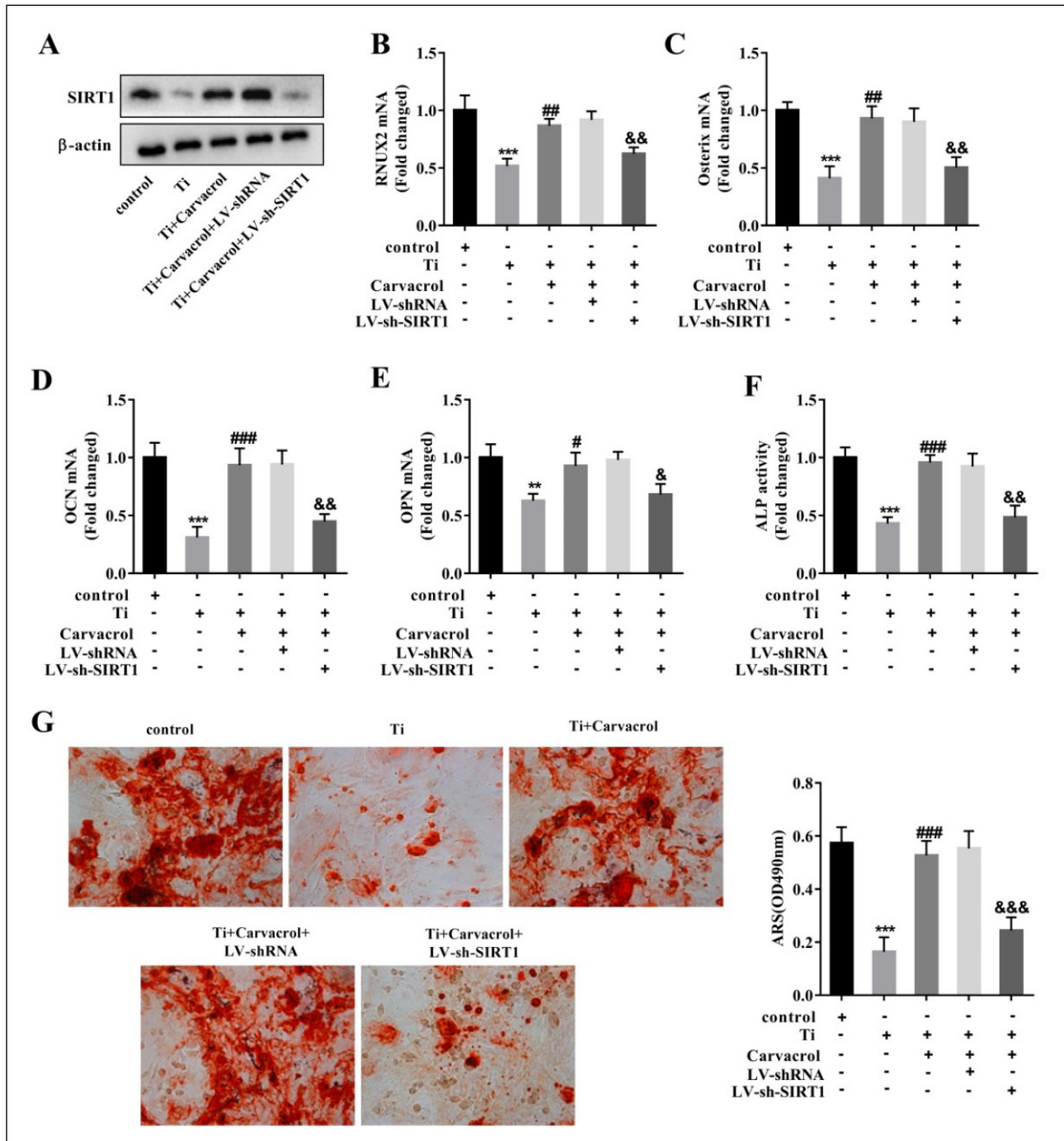
Figure 3. Carvacrol alleviates osteogenic differentiation of Ti-inhibited BMSCs by upregulating SIRT1. BMSCs were transfected with LV-sh-SIRT1 or LV-shRNA (negative control), then cultured for osteogenic differentiation after transfection and treated with carvacrol (25 μM). (**A**) Expression levels of SIRT1 were analyzed by Western blotting. (**B-E**) RUNX2, Osterix, OCN, and OPN mRNA expression in mouse BMSCs was measured by RT-qPCR. (**F**) Quantitative analysis of ALP activity in BMSCs. (**G**) Mineralized nodules were measured by ARS staining. Mineralized nodules were quantified by calculating the ratio of mineralized area to total area after staining. One-way ANOVA was performed by Tukey's multiple comparison test, and statistically significant differences are indicated by: $**P < 0.01$, $***P < 0.001$ vs. the control group; $^{\#}P < 0.05$, $^{\#\#}P < 0.01$, $^{\#\#\#}P < 0.001$ *vs*. Ti group; $^{\&}P < 0.05$, $^{\&\&}P < 0.01$, $^{\&\&\&}P < 0.001$ *vs*. Ti + Carvacrol + LV-shRNA group.

upregulation of SIRT1 expression induced by carvacrol.

NEAT1 stabilizes the expression of SIRT1 by inhibiting its ubiquitination levels

Previous studies have shown that lncRNAs can regulate the expression of SIRT1 through ubiquitination pathways [45-47]. Based on this evidence, we hypothesized that NEAT1 may modulate SIRT1 expression through ubiquitination. To investigate this hypothesis, we used cyclohexi-

mide (CHX) treatment to evaluate the effect of NEAT1 on SIRT1 protein stability. BMSCs were transfected with LV-NEAT1 plasmid followed by treatment with 10μg/mL CHX for 0, 3, 6, and 9 hours. Our results showed that NEAT1 overexpression significantly inhibited the time-dependent degradation of SIRT1 protein in BMSCs under CHX treatment (Figure 5A). Next, BMSCs were treated with (or without) 10 μM proteasome inhibitor MG132 for 4 hours. Western blot analysis showed that MG132 sig-
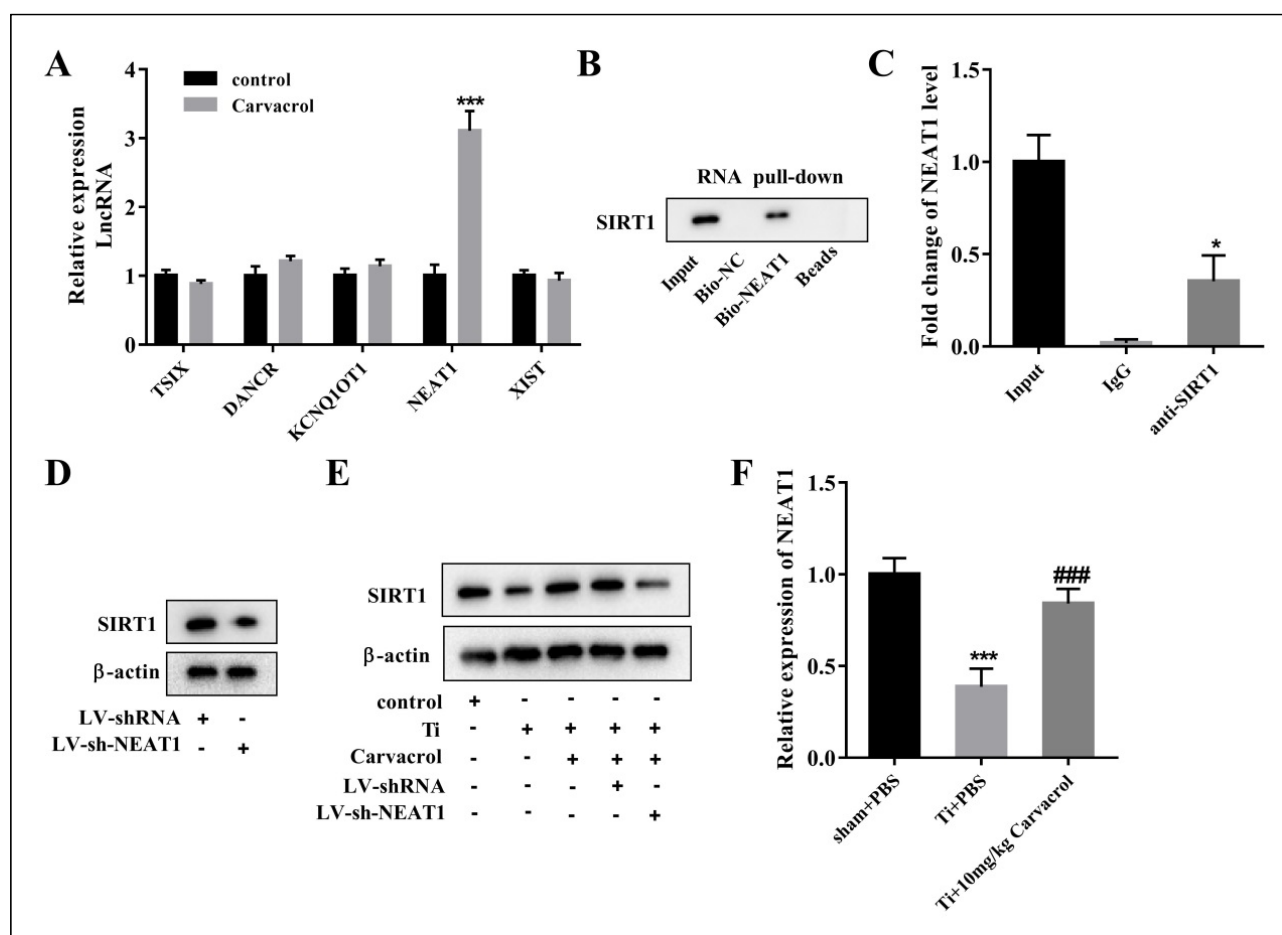
Figure 4. Carvacrol promotes SIRT1 expression through NEAT1. (**A**) The mRNA levels of lncRNAs, including TSIX, DANCR, KCNQ1OT1, NEAT1, and XIST, in carvacrol-treated cells were measured by RT-PCR. ***$P < 0.001$ *vs.* control. Statistical analysis was performed by two-tailed unpaired Student's t-test. (**B**) RNA pull-down assay was performed to verify the interaction between NEAT1 and SIRT1. (**C**) The binding between NEAT1 and SIRT1 was measured using RIP assay. *$P < 0.05$ *vs.* IgG. (**D**) Protein levels of SIRT1 in BMSCs transfected with LV-sh-SIRT1 or LV-shRNA were determined by Western blot assays. (**E**) BMSCs were divided into control, Ti, Ti + Carvacrol, Ti + Carvacrol + LV-shRNA, and Ti + Carvacrol + LV-sh-NEAT1 groups. SIRT1 protein levels were detected by Western blotting. (**F**) NEAT1 mRNA expression levels in the calvarial samples in Figure 1 were detected by RT-qPCR. One-way ANOVA was performed by Tukey's multiple comparison test, and statistically significant differences are indicated by: ***$P < 0.001$ *vs.* sham + PBS group; ###$P < 0.001$ *vs.* Ti + PBS group.

nificantly increased the protein level of SIRT1, confirming the successful blockade of proteasome-mediated protein degradation (Figure 5B). In the absence of MG132 treatment, NEAT1 overexpression resulted in a significant increase in SIRT1 protein levels. However, when BMSCs were pretreated with MG132, the effect of LV-NEAT1 on SIRT1 protein levels was relatively modest. This observation supports the notion that the effect of NEAT1 on SIRT1 is dependent on proteasome-mediated degradation (Figure 5B). The ubiquitination assay further confirmed that NEAT1 overexpression inhibited the ubiquitination modification of SIRT1 (Figure 5C). According to the literature, the E3 ubiquitin ligase SMURF2 interacts with SIRT1 and facilitates its ubiquitination and degradation [48]. We hypothesized that NEAT1 regulates the ubiquitination levels of SIRT1 by modulating the interaction between SIRT1 and SMURF2. The IP and IB assay revealed a significant decrease in the enrichment of SIRT1 within the SMURF2 immunoprecipitation complex in BMSCs transfected with LV-NEAT1 (Figure 5D). Overall, these results suggest that NEAT1 plays a pivotal role in stabilizing SIRT1 and effectively inhibiting its ubiquitination

modification levels.

Carvacrol promotes SIRT1 expression by upregulating NEAT1 and alleviates Ti-inhibited osteoblast differentiation

We first examined the expression levels of NEAT1, SIRT1, and osteogenic differentiation-related factors in BMSCs after different treatments. The results showed that knockdown of NEAT1 significantly inhibited the carvacrol-induced increase in NEAT1 expression, providing compelling evidence for the efficacy of transfection (Figure 6A). Furthermore, LV-sh-NEAT1 suppressed the carvacrol-promoted expression of SIRT1, RUNX2, Osterix, OCN, and OPN, whereas LV-SIRT1 reversed the effects of LV-sh-NEAT1 (Figure 6B-F). Next, we performed osteogenic differentiation of BMSCs in different treatment groups. The ALP activity was significantly increased in the Ti + Carvacrol group, while the Ti + Carvacrol + LV-sh-NEAT1 group showed a significant decrease. As expected, ALP activity increased again in the Ti+Carvacrol+LV-sh-NEAT1+LV-SIRT1 group (Figure 6G). The ARS staining results showed enhanced mineralization ability in BMSCs
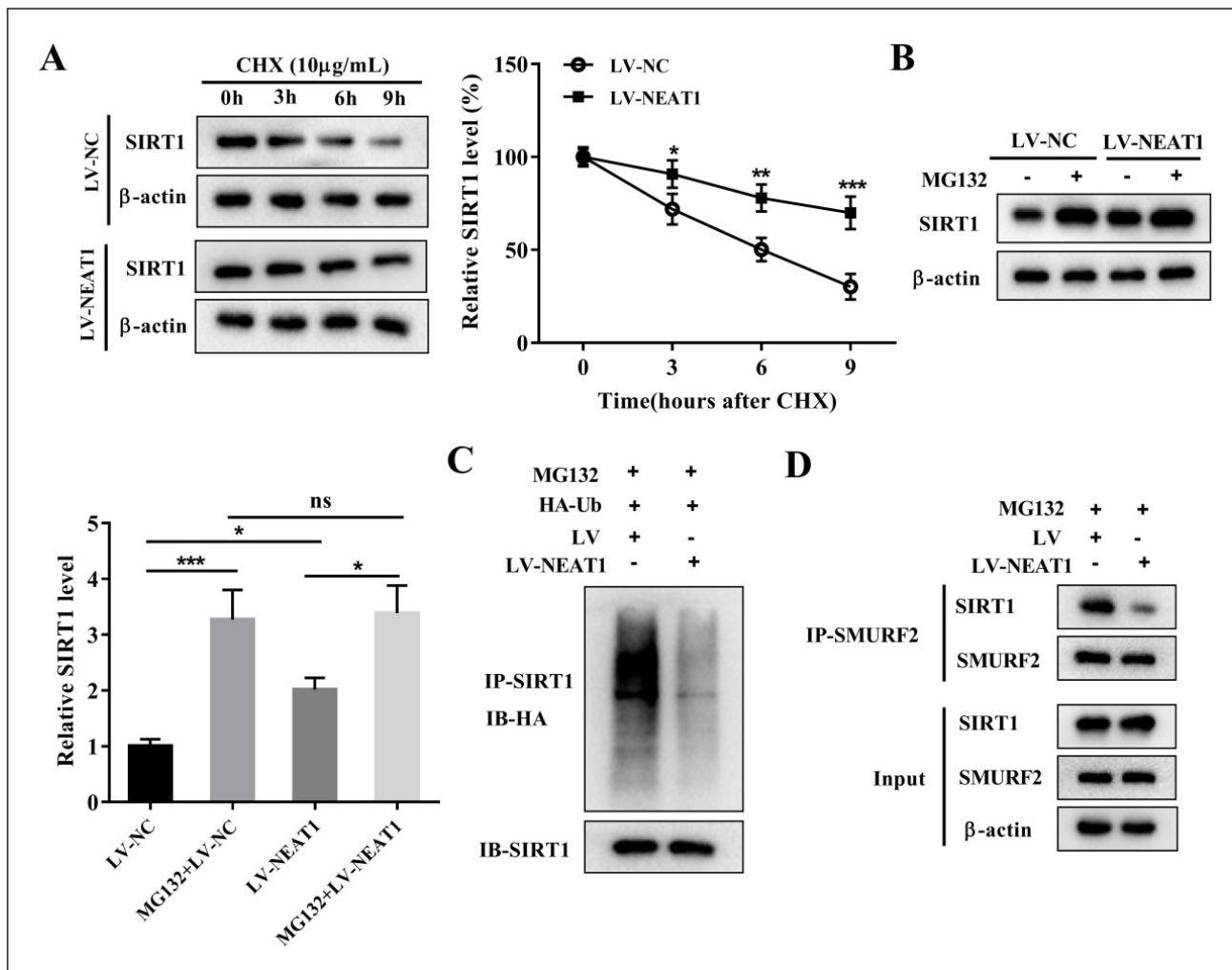
Figure 5. NEAT1 stabilizes the expression of SIRT1 by inhibiting its ubiquitination levels. BMSCs were transfected with LV-NEAT1 or LV-NC. (**A**) BMSCs treated with CHX for 0, 3, 6, and 9 h were analyzed for SIRT1 expression by Western blotting. *$P < 0.05$, **$P < 0.01$, ***$P < 0.001$ *vs*. control. Two-way ANOVA was performed by Bonferroni's multiple comparison test. (**B**) BMSCs were treated with (or without) 10 μM proteasome inhibitor MG132 for 4 h. Cells were harvested and SIRT1 protein expression was detected by Western blotting. One-way ANOVA was performed by Tukey's multiple comparison test, and statistically significant differences are indicated by: *$P < 0.05$, ***$P < 0.001$. One-way ANOVA with Tukey's multiple comparison test. (**C**) After MG132 (10 μM) treatment for 4 h, IP assays were performed with anti-SIRT1 in BMSCs transfected with LV-NEAT1 or LV-NC. IB analysis of total Ub and SIRT1 in SIRT1-immunoprecipitated products was performed. (**D**) The interaction between SIRT1 and SMURF2 regulated by NEAT1 was analyzed by IP and IB assay.

of the Ti + Carvacrol group, whereas decreased mineralization ability was observed in the Ti + Carvacrol + LV-sh-NEAT1 group. After transfection with LV-SIRT1, the mineralization ability was restored (Figure 6H). These results demonstrate that silencing of NEAT1 can inhibit the osteogenic effect of carvacrol, but this inhibition can be reversed by overexpression of SIRT1.

Carvacrol alleviates osteolysis in aged mice by upregulating NEAT1

We randomly divided 18-month-old mice into four groups: Ti + PBS, Ti + Carvacrol, Ti + Carvacrol + LV-shRNA, and Ti + Carvacrol + LV-sh-NEAT1 groups. Two weeks after surgery, we collected calvarial tissue from the mice and performed micro-CT scanning, quantitative micro-CT analysis, and Western blotting. Analysis of the three-dimensional reconstructed images revealed extensive erosion and reduced thickness of the calvarial bone in the Ti + PBS group. However, application of carvacrol

ameliorated calvarial erosion, and injection of LV-sh-NEAT1 partially reversed the effects of carvacrol (Figure 7A). Furthermore, carvacrol also upregulated bone density and BV/TV levels, which were partially counteracted by LV-sh-NEAT1 injection (Figure 7B-C). This suggests that NEAT1 may play a critical role in mediating the protective effects of carvacrol on calvarial bone erosion. Additionally, LV-sh-NEAT1 attenuated the carvacrol-induced increase in the protein levels of SIRT1, RUNX2, Osterix, OCN, and OPN (Figure 7D). These findings demonstrate that carvacrol alleviates osteolysis in aged mice by upregulating NEAT1.

Discussion

This study demonstrated the potential bone-protective effects of carvacrol. Carvacrol enhances SIRT1 expression by upregulating NEAT1, thereby alleviating the inhibitory
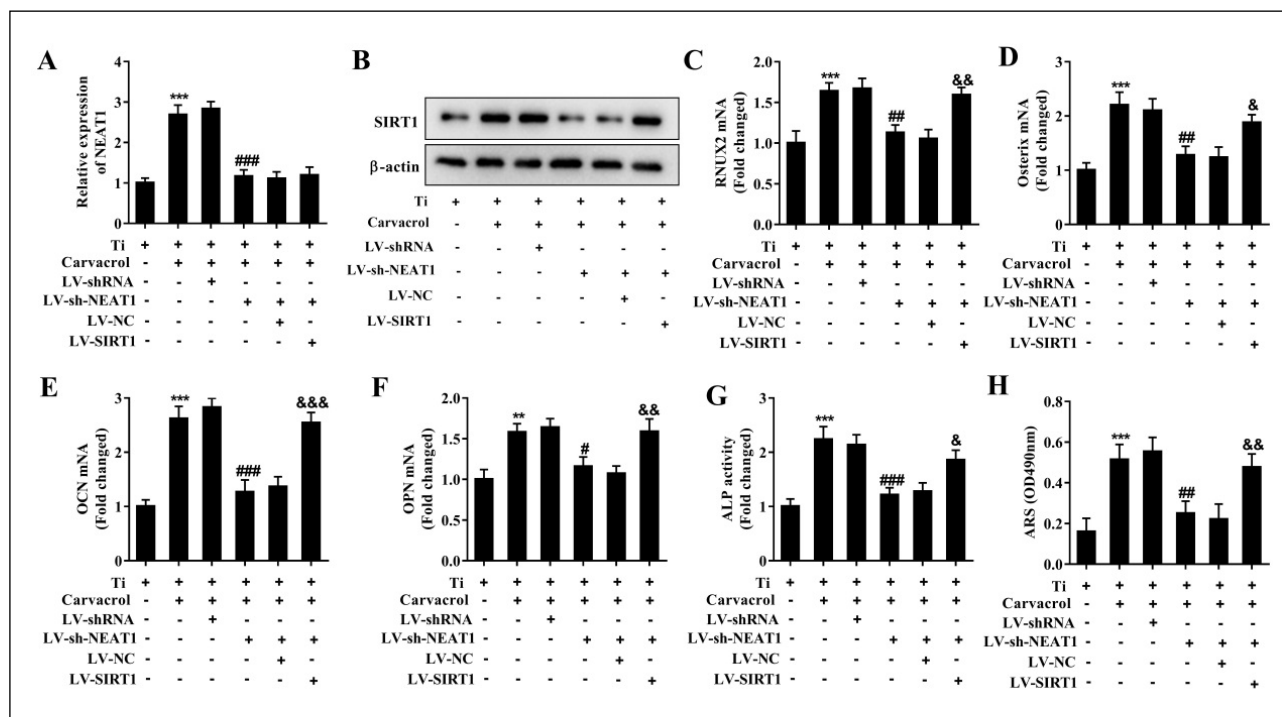
Figure 6. Carvacrol promotes SIRT1 expression by upregulating NEAT1 and alleviates Ti-inhibited osteoblast differentiation. BMSCs were transfected with LV-shRNA, LV-sh-NEAT1, LV-sh-NEAT1 + LV-NC or LV-sh-NEAT1 + LV-SIRT1, then cultured for osteogenic differentiation after transfection and treated with carvacrol (25 μM). (**A**) RT-qPCR was performed to analyze the expression of NEAT1. (**B**) Protein expression of SIRT1 was examined by Western blotting. β-Actin was used as an internal control for equal amounts of protein applied. (**C-F**) Reverse transcription-quantitative PCR was performed to analyze the expression of RUNX2, Osterix, OCN, and OPN. (**G**) Quantitative analysis of ALP activity of BMSCs. (H) ARS staining measured mineralized nodules. Mineralized nodules were quantified by calculating the ratio of mineralized area to total area after staining. One-way ANOVA was performed by Tukey's multiple comparison test, and statistically significant differences are indicated by: **$P < 0.01$, ***$P < 0.001$ vs. Ti group; #$P < 0.05$, ##$P < 0.01$, ###$P < 0.001$ *vs*. Ti + Carvacrol + LV-shRNA group; &$P < 0.05$, &&$P < 0.01$, &&&$P < 0.001$ *vs*. Ti + Carvacrol + LV-sh-NEAT1 + LV-NC group.

effect of titanium particles on osteoblast differentiation. In summary, carvacrol may have potential therapeutic effects on osteolysis in aged mice by promoting osteogenic differentiation of BMSCs. This finding provides a promising direction for the development of new treatment strategies and drugs (Figure 8).

Osteolysis refers to a pathological condition characterized by increased bone resorption and decreased bone formation in bone tissue, resulting in destruction and loss of bone mass [49]. This pathological process is typically triggered by wear particles following joint replacement surgery [6]. The probability of wear particle-induced osteolysis is significantly higher in elderly patients [50]. Therefore, inducing osteogenesis promotion may be one of the most promising therapeutic approaches to treat osteolysis. BMSCs have the potential for osteogenic differentiation, which can promote bone formation and repair by differentiating into osteoblasts and osteocytes [51, 52]. Therefore, the development of drugs that enhance the osteogenic differentiation capacity of BMSCs offers a new therapeutic approach for the treatment of osteolysis. Previous studies have revealed the potential regulatory effects of carvacrol on osteoblasts and osteoclasts [18, 21]. Additionally, carvacrol has been suggested to reduce tissue damage and bone loss caused by ligature-induced periodontitis [53, 20]. However, the potential of carvacrol in regulating osteogenic differentiation for the treatment of particle-induced osteolysis has not been explored until now.

In this study, we demonstrated for the first time that carvacrol attenuated particle-induced osteolysis in an osteolysis model of aged mice. It is worth noting that the accumulation of wear particles (Ti particles) around implants can lead to local bone resorption and ultimately calvarial erosion [54, 55]. As expected, micro-CT imaging, bone density and BV/TV statistical analysis showed that carvacrol exhibited a protective effect against Ti-induced bone destruction. Furthermore, a recent study by Spalletta *et al*. reported the involvement of carvacrol in the differentiation of umbilical cord mesenchymal stem cells [22]. Therefore, in this study, we also evaluated the effect of carvacrol on the osteogenic differentiation and osteogenesis of titanium-inhibited BMSCs. The results showed that titanium treatment suppressed cell mineralization, activity of osteogenic differentiation marker ALP, and expression of osteogenic differentiation-related factors (RUNX2, Osterix, OCN, and OPN). However, carvacrol was able to reverse these effects induced by titanium.

The reduction of SIRT1 levels and activity is associated with the progression of osteolysis [24, 25, 56, 57]. Furthermore, SIRT1 is involved in the differentiation of BMSCs in aged mice and promotes bone formation [58, 59]. SIRT1 effectively improves osteolysis by enhancing the osteogenic potential of BMSCs [27]. Our research showed that carvacrol upregulates SIRT1 levels, which is consistent with previous findings [34]. A previous study
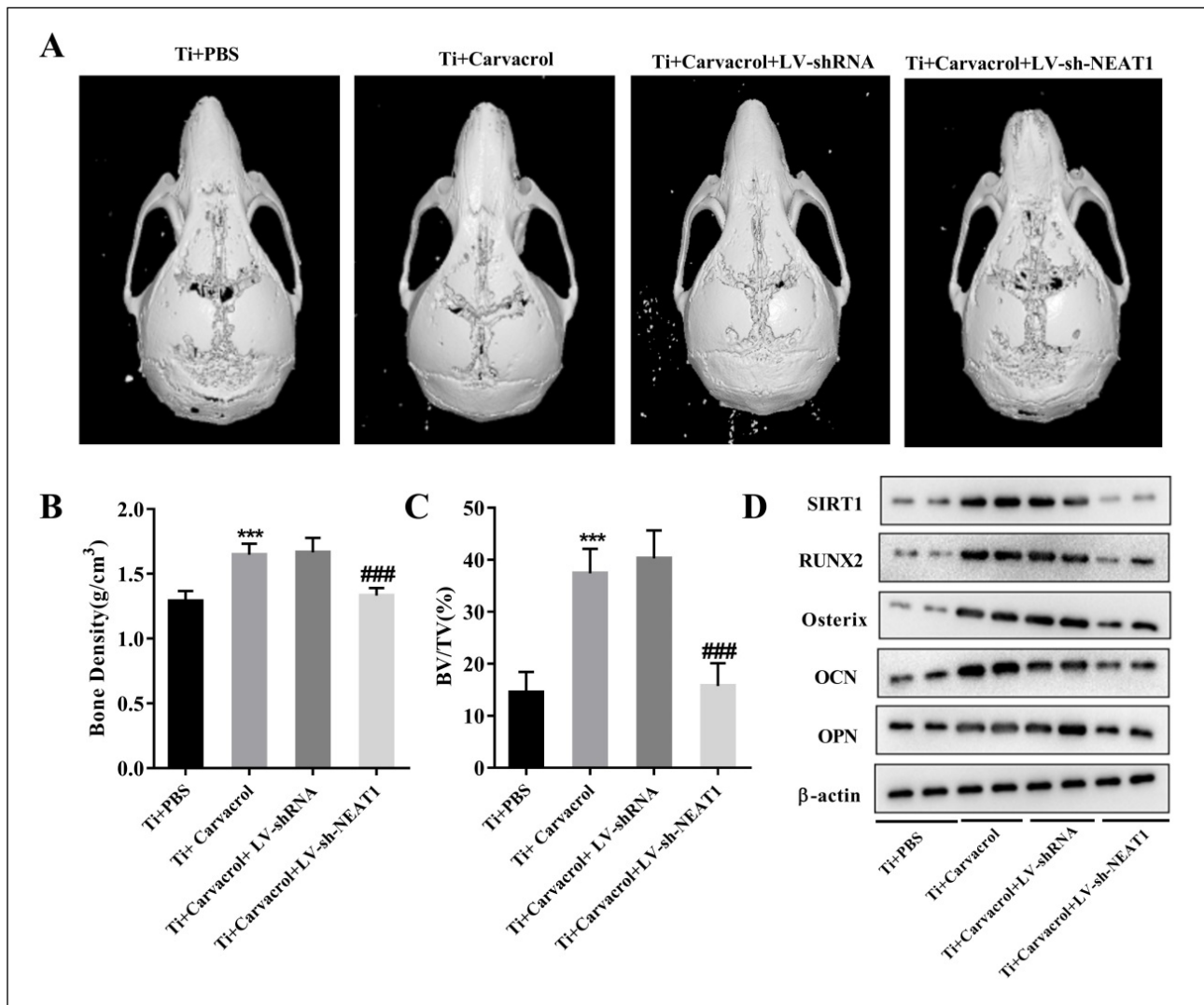
Figure 7. Carvacrol alleviates osteolysis in aged mice by upregulating NEAT1. We randomly divided 18-month-old mice into four groups: Ti + PBS, Ti + Carvacrol, Ti + Carvacrol + LV-shRNA, and Ti + Carvacrol + LV-sh-NEAT1 groups. Two weeks after surgery, we collected calvarial tissues from the mice and performed micro-CT scanning, quantitative micro-CT analysis, and Western blotting. (**A**) Representative micro-CT three-dimensional reconstructed images of mouse calvaria in each group. (**B-C**) Bone density (g/cm³) and BV/TV (%) of each group were measured. One-way ANOVA was performed by Tukey's multiple comparison test, and statistically significant differences are indicated by: ***$P < 0.001$ vs. Ti + PBS group; ###$P < 0.001$ *vs.* Ti + Carvacrol + LV-shRNA group. (**D**) Protein expression of SIRT1, RUNX2, Osterix, OCN, and OPN was examined by Western blotting. β-Actin was used as an internal control for equal amounts of protein applied.

showed that melatonin promotes the osteogenic potential of BMSCs by regulating SIRT1-mediated antioxidant properties [29]. Eldecalcitol inhibits BMSC senescence by modulating the SIRT1-Nrf2 pathway [60]. Based on these findings, we further investigate whether carvacrol regulates SIRT1 to influence the osteogenic differentiation of BMSCs. The inhibitory effect of sh-SIRT1 on carvacrol-induced osteogenic differentiation of BMSCs was confirmed by ALP activity assay, ARS staining, and RT-qPCR analysis.

Many studies have highlighted the critical impact of lncRNAs on various processes. Increasing evidence suggests that lncRNAs are involved in BMSC osteogenic differentiation [61], bone formation [62], and osteoblast matrix mineralization [63]. To gain a deeper understanding of the molecular mechanism by which carvacrol regulates osteolysis, we screened several lncRNAs potentially involved in SIRT1 interaction and osteolysis. Surprisingly,

only NEAT1 expression was regulated by the addition of carvacrol to the culture medium. LncRNA NEAT1 was found to activate BTK and regulate the NF-κB pathway, thereby participating in the process of wear particle-induced osteolysis [64]. Our results also show that inhibition of NEAT1 attenuates the protective effect of carvacrol on calvarial bone and is involved in osteolysis. LncRNAs can be involved in the regulation of gene expression through various mechanisms [65, 66], including the regulation of SIRT1 through ubiquitination [67, 46, 47]. To further investigate the relationship between NEAT1 and SIRT1, we performed RNA pull-down and RIP experiments. We found that NEAT1 stabilizes SIRT1 expression by inhibiting its ubiquitination modification. In addition, NEAT1 has been shown to promote osteogenic differentiation of human bone marrow mesenchymal stem cells [39]. The results of our study indicate that in Ti-induced in vitro BMSCs, LV-sh-NEAT1 inhibits the osteogenic differentia-
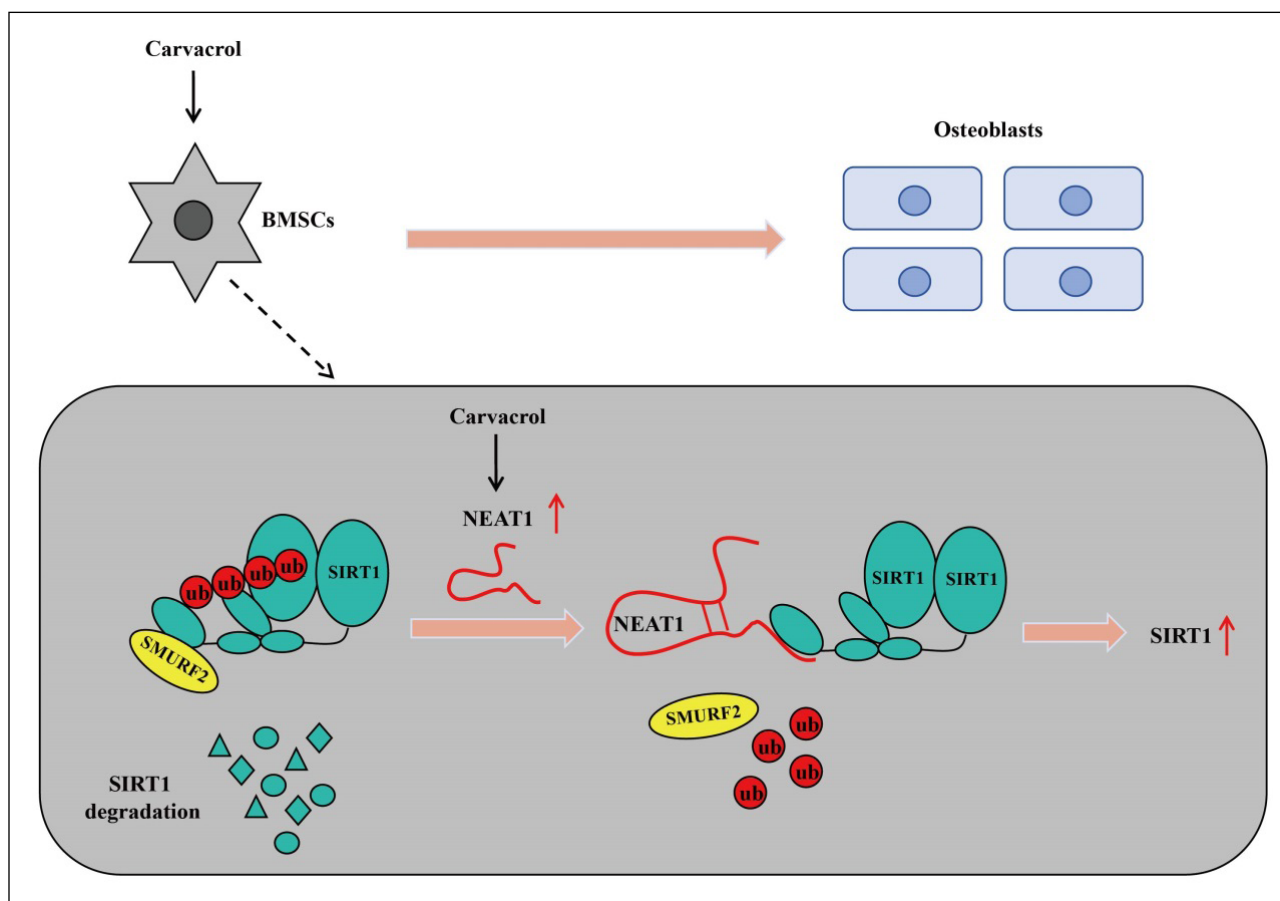
Figure 8. A working model has been proposed for carvacrol to induce osteogenic differentiation of BMSCs and alleviate osteolysis in aged mice. Carvacrol promotes SIRT1 expression by upregulating NEAT1 and induces the expression of transcription factors, ultimately leading to the promotion of osteogenic differentiation of bone marrow mesenchymal stem cells and the alleviation of osteolysis in aged mice.

tion promoted by carvacrol, while LV-SIRT1 reverses the effect of sh-NEAT1.

Conclusions

In conclusion, carvacrol promotes SIRT1 expression by upregulating NEAT1 and induces the expression of osteogenesis-related transcription factors. This mechanism may contribute to the promotion of osteogenic differentiation of BMSCs and the alleviation of osteolysis. However, this study has only been discussed in animal models, and there is a lack of further clinical research evidence.

Declarations

References

1. Ryu KJ. CORR Insights®: what host factors affect aseptic loosening after THA and TKA? *Clin Orthop Relat Res*, 2015, 473(8): 2710-2711. [Crossref]
2. Heyse TJ, Ries MD, Bellemans J, Goodman SB, Scott RD, Wright TM, *et al*. Total knee arthroplasty in patients with juvenile idiopathic arthritis. *Clin Orthop Relat Res*, 2014, 472(1): 147-154. [Crossref]
3. Sculco TP. The role of constraint in total knee arthoplasty. *J Arthroplasty*, 2006, 21(4 Suppl 1): 54-56. [Crossref]
4. Oussedik S, Abdel MP, Cross MB, & Haddad FS. Alignment and fixation in total knee arthroplasty: changing paradigms. *Bone Joint J*, 2015, 97-b (10 Suppl A): 16-19.[Crossref]
5. Dong J, Zhang L, Ruan B, Lv Z, Wang H, Wang Y, *et al*. NRF2 is a critical regulator and therapeutic target of metal implant particle-incurred bone damage. *Biomaterials*, 2022, 288: 121742. [Crossref]
6. Goodman SB. Wear particles, periprosthetic osteolysis and the immune system. *Biomaterials*, 2007, 28(34): 5044-5048. [Crossref]

7. Yao J, Cs-Szabó G, Jacobs J, Kuettner KE, & Glant TT. Suppression of osteoblast function by titanium particles. *J Bone Joint Surg Am*, 1997, 79(1): 107-112. [Crossref]

8. Pioletti DP, Takei H, Kwon SY, Wood D, & Sung KL. The cytotoxic effect of titanium particles phagocytosed by osteoblasts. *J Biomed Mater Res*, 1999, 46(3): 399-407.[Crossref]

9. Zhang Y, Lin Y, Xiao L, Feng E, Wang W, & Lin L. The effects of icariine concentration on osteoclasts bone resorption induced by titanium particles in vitro. *Regen Biomater*, 2015, 2(3): 197-202. [Crossref]

10. Liu G, Liu N, Xu Y, Ti Y, Chen J, Chen J, *et al*. Endoplasmic reticulum stress-mediated inflammatory signaling pathways within the osteolytic periosteum and interface membrane in particle-induced osteolysis. *Cell Tissue Res*, 2016, 363(2): 427-447. [Crossref]

11. Zaher W, Harkness L, Jafari A, & Kassem M. An update of human mesenchymal stem cell biology and their clinical uses. *Arch Toxicol*, 2014,88(5):1069-1082. [Crossref]

12. Al-Ahmari F, Al-Rasheed A, Ramalingam S, Aldahmash A, Nooh N, Wang CY, *et al*. Efficacy of mesenchymal stem cells as adjunct to guided bone regeneration in standardized calvarial defects in rats: an in vivo microcomputed tomographic and histologic analysis. *Int J Periodontics Restorative Dent*, 2016, 36 Suppl: s23-37. [Crossref]

13. Namli H, Erdogan Ö, Gönlüşen G, Kahraman OE, Aydin HM, Karabag S, *et al*. Vertical bone augmentation using bone marrow-derived stem cells: an in vivo study in the rabbit calvaria. *Implant Dent*, 2016, 25(1): 54-62. [Crossref]

14. Su P, Tian Y, Yang C, Ma X, Wang X, Pei J, *et al*. Mesenchymal stem cell migration during bone formation and bone diseases therapy. *Int J Mol Sci*, 2018, 19(8): 2343-2350. [Crossref]

15. Choudhery MS, Khan M, Mahmood R, Mehmood A, Khan SN, & Riazuddin S. Bone marrow derived mesenchymal stem cells from aged mice have reduced wound healing, angiogenesis, proliferation and anti-apoptosis capabili-ties. *Cell Biol Int*,2012,36(8):747-753. [Crossref]

16. De Vincenzi M, Stammati A, De Vincenzi A, & Silano M. Constituents of aromatic plants: carvacrol. *Fitoterapia*, 2004, 75(7-8): 801-804. [Crossref]

17. Baser KH. Biological and pharmacological activities of carvacrol and carvacrol bearing essential oils. *Curr Pharm Des*, 2008, 14(29): 3106-3119. [Crossref]

18. Deepak V, Kasonga A, Kruger MC, & Coetzee M. Carvacrol inhibits osteoclastogenesis and negatively regu-lates the survival of mature osteoclasts. *Biol Pharm Bull*, 2016, 39(7): 1150-1158. [Crossref]

19. Botelho MA, Martins JG, Ruela RS, I R, Santos JA, Soares JB, *et al*. Protective effect of locally applied carvacrol gel on ligature-induced periodontitis in rats: a tapping mode AFM study. *Phytother Res*, 2009, 23(10): 1439-1448. [Crossref]

20. Kuo PJ, Hung TF, Lin CY, Hsiao HY, Fu MW, Hong PD, *et al*. Carvacrol ameliorates ligation-induced periodontitis in rats. *J Periodontol*, 2017, 88(7): e120-e128. [Crossref]

21. Vu AA, & Bose S. Natural antibiotic oregano in hydroxyapatite-coated titanium reduces osteoclastic bone resorp tion for orthopedic and dental applications. *ACS Appl Mater Interfaces*, 2020, 12(47): 52383-52392. [Crossref]

22. Spalletta S, Flati V, Toniato E, Di Gregorio J, Marino A, Pierdomenico L, *et al*. Carvacrol reduces adipogenic differentiation by modulating autophagy and ChREBP expression. *PLoS One*, 2018, 13(11): e0206894. [Crossref]

23. Matluobi D, Araghi A, Maragheh BFA, Rezabakhsh A, Soltani S, Khaksar M, *et al*. Carvacrol promotes angiogenic paracrine potential and endothelial differentiation of human mesenchymal stem cells at low concentrations. *Microvasc Res*, 2018, 115: 20-27. [Crossref]

24. Deng Z, Jin J, Wang Z, Wang Y, Gao Q, & Zhao J. The metal nanoparticle-induced inflammatory response is regulated by SIRT1 through NF-κB deacetylation in aseptic loosening. *Int J Nanomedicine*, 2017, 12: 3617-3636. [Crossref]

25. Deng Z, Wang Z, Jin J, Wang Y, Bao N, Gao Q, *et al*. SIRT1 protects osteoblasts against particle-induced inflammatory responses and apoptosis in aseptic prosthesis loosening. *Acta Biomater*, 2017, 49: 541-554. [Crossref]

26. Liu L, Zhou M, Zhu R, Zhou J, Ni L, Wang Z, *et al*. Hydrogen sulfide protects against particle-induced inflammatory response and osteolysis via SIRT1 pathway in prosthesis loosening. *Faseb j*, 2020, 34(3): 3743-3754. [Crossref]

27. Zhang Y, Zhu X, Wang G, Chen L, Yang H, He F, *et al*. Melatonin rescues the Ti particle-impaired osteogenic potential of bone marrow mesenchymal stem cells via the SIRT1/SOD2 signaling pathway. *Calcif Tissue Int*, 2020, 107(5): 474-488. [Crossref]

28. Wang Y, Chen G, Yan J, Chen X, He F, Zhu C, *et al*. Upregulation of SIRT1 by kartogenin enhances antioxidant functions and promotes osteogenesis in human mesenchymal stem cells. *Oxid Med Cell Longev*, 2018, 2018: 1368142. [Crossref]

29. Chen W, Chen X, Chen AC, Shi Q, Pan G, Pei M, *et al*. Melatonin restores the osteoporosis-impaired osteogenic potential of bone marrow mesenchymal stem cells by preserving SIRT1-mediated intracellular antioxidant properties. *Free Radic Biol Med*, 2020, 146: 92-106. [Crossref]

30. Satija NK, Gurudutta GU, Sharma S, Afrin F, Gupta P, Verma YK, *et al*. Mesenchymal stem cells: molecular targets for tissue engineering. *Stem Cells Dev*, 2007, 16(1): 7-23. [Crossref]

31. Tseng PC, Hou SM, Chen RJ, Peng HW, Hsieh CF, Kuo ML, *et al*. Resveratrol promotes osteogenesis of human mesenchymal stem cells by upregulating RUNX2 gene expression via the SIRT1/FOXO3A axis. *J Bone Miner Res*, 2011, 26(10): 2552-2563. [Crossref]

32. Terauchi K, Kobayashi H, Yatabe K, Yui N, Fujiya H, Niki H, *et al*. The NAD-dependent deacetylase sirtuin-1 regulates the expression of osteogenic transcriptional activator runt-related transcription factor 2 (Runx2) and production of matrix metallopr-oteinase (MMP)-13 in chondrocytes in osteoarthritis. *Int J Mol Sci*, 2016, 17(7): 1019-1022. [Crossref]

33. Zainabadi K, Liu CJ, & Guarente L. SIRT1 is a positi-ve regulator of the master osteoblast transcription fa-

ctor RUNX2. *PLoS One*, 2017,12(5): e0178520. [Crossref]

34. Kim E, Choi Y, Jang J, & Park T. Carvacrol protects against hepatic steatosis in mice fed a high-fat diet by enhancing SIRT1-AMPK signaling. *Evid Based Complement Alternat Med*, 2013, 2013: 290104. [Crossref]

35. Fatica A, & Bozzoni I. Long non-coding RNAs: new players in cell differentiation and development. *Nat Rev Genet*, 2014, 15(1): 7-21. [Crossref]

36. Bu Y, Zheng D, Wang L, & Liu J. LncRNA TSIX promotes osteoblast apoptosis in particle-induced osteolysis by down-regulating miR-30a-5p. *Connect Tissue Res*, 2018, 59(6): 534-541. [Crossref]

37. Tang Z, Gong Z, & Sun X. LncRNA DANCR involved osteolysis after total hip arthroplasty by regulating FOXO1 expression to inhibit osteoblast differentiation. *J Biomed Sci*, 2018, 25(1): 4-11. [Crossref]

38. Gao X, Ge J, Li W, Zhou W, & Xu L. LncRNA KCNQ1OT1 ameliorates particle-induced osteolysis through inducing macrophage polarization by inhibiting miR-21a-5p. *Biol Chem*,2018,399(4): 375-386. [Crossref]

39. Zhang Y, Chen B, Li D, Zhou X, &Chen Z. LncRNA NEAT1/miR-29b-3p/BMP1 axis promotes osteogenic differentiation in human bone marrow-derived mesenchymal stem cells. *Pathol Res Pract*, 2019, 215(3): 525-531. [Crossref]

40. Zheng C, Bai C, Sun Q, Zhang F, Yu Q, Zhao X, *et al*. Long noncoding RNA XIST regulates osteogenic differentiation of human bone marrow mesenchymal stem cells by targeting miR-9-5p. *Mech Dev*, 2020, 162: 103612. [Crossref]

41. Kaar SG, Ragab AA, Kaye SJ, Kilic BA, Jinno T, Goldberg VM, *et al*. Rapid repair of titanium particle-induced osteolysis is dramatically reduced in aged mice. *J Orthop Res*, 2001, 19(2): 171-178. [Crossref]

42. Johnson C, Zhu L, Mangalindan R, Whitson J, Sweetwyne M, Valencia AP, *et al*. Older-aged C57BL/6 mice fed a diet high in saturated fat and sucrose for ten months show decreased resilience to aging. *Aging Pathobiology and Therapeutics*, 2023, 5(3): 101-106. [Crossref]

43. Gu M, Pan B, Chen W, Xu H, Wu X, Hu X, *et al*. SPHK inhibitors and zoledronic acid suppress osteoclastogenesis and wear particle-induced osteolysis. *Front Pharmacol*, 2021, 12: 794429. [Crossref]

44. Li X, Wang X, Zhang C, Wang J, Wang S, & Hu L. Dysfunction of metabolic activity of bone marrow mesenchymal stem cells in aged mice. *Cell Prolif*, 2022, 55(3): e13191.[Crossref]

45. Tang Y, Ma N, Luo H, Chen S, & Yu F. Downregulated long non-coding RNA LINC01093 in liver fibrosis promotes hepatocyte apoptosis via increasing ubiquitination of SIRT1.*J Biochem*,2020,168(3):315-320. [Crossref]

46. Shi C, Zheng W, &Wang J. LncRNA-CRNDE regulates BMSC chondrogenic differentiation and promotes cartilage repair in osteoarthritis through SIRT1/SOX9. *Mol Cell Biochem*, 2021, 476(4): 1881-1890. [Crossref]

47. Zhang J, Chen C, Zhang S, Chen J, Wu L, & Chen Z. LncRNA XIST restrains the activation of Müller cells and inflammation in diabetic retinopathy via stabilizing SIRT1. *Autoimmunity*, 2021, 54(8): 504-513. [Crossref]

48. Yu L, Dong L, Li H, Liu Z, Luo Z, Duan G, *et al*. Ubiquitination-mediated degradation of SIRT1 by SMURF2 suppresses CRC cell proliferation and tumorigenesis. *Oncogene*, 2020, 39(22): 4450-4464. [Crossref]

49. Alhasan H, Terkawi MA, Matsumae G, Ebata T, Tian Y, Shimizu T, *et al*. Inhibitory role of Annexin A1 in pathological bone resorption and therapeutic implications in periprosthetic osteolysis. *Nat Commun*, 2022, 13(1): 3919-3922. [Crossref]

50. Yamada C, Ho A, Akkaoui J, Garcia C, Duarte C, & Movila A. Glycyrrhizin mitigates inflammatory bone loss and pro-motes expression of senescence-protective sirtuins in an aging mouse model of periprosthetic osteolysis. *Biomed Pharmacother*, 2021, 138: 111503. [Crossref]

51. He Z, Li H, Han X, Zhou F, Du J, Yang Y, *et al*. Irisin inhibits osteocyte apoptosis by activating the Erk signaling pathway in vitro and attenuates ALCT-induced osteoarthritis in mice. *Bone*, 2020, 141: 115573. [Crossref]

52. Wu S, Zhang L, Zhang R, Yang K, Wei Q, Jia Q, *et al*. Rat bone marrow mesenchymal stem cells induced by rrPDGF-BB promotes bone regeneration during distraction osteogenesis. *Front Bioeng Biotechnol*, 2023, 11: 1110703. [Crossref]

53. Botelho MA, Rao VS, Montenegro D, Bandeira MA, Fonseca SG, Nogueira NA, *et al*. Effects of a herbal gel containing carvacrol and chalcones on alveolar bone resorption in rats on experimental periodontitis. *Phytother Res*, 2008, 22(4): 442-449. [Crossref]

54. Shi J, Gu Y, Wang Y, Bai J, Xiong L, Tao Y, *et al*. Inhibitory effect of acetyl-11-keto-β-boswellic acid on titanium particle-induced bone loss by abrogating osteoclast formation and downregulating the ERK signaling pathway. *Int Immunopharmacol*, 2021, 94: 107459. [Crossref]

55. Jiao Z, Chai H, Wang S, Sun C, Huang Q, & Xu W. SOST gene suppression stimulates osteocyte Wnt/β-catenin signaling to prevent bone resorption and attenuates particle-induced osteolysis. *J Mol Med (Berl)*, 2023, 101(5): 607-617. [Crossref]

56. Zhang L, Bao D, Li P, Lu Z, Pang L, Chen Z, *et al*. Particle-induced SIRT1 downregulation promotes osteoclastogenesis and osteolysis through ER stress regulation. *Biomed Pharmacother*, 2018, 104: 300-306. [Crossref]

57. Zhang L, Zhao W, Bao D, Sun K, Li P, Gao Z, *et al*. miR-9-5p promotes wear-particle-induced osteoclast-ogenesis through activation of the SIRT1/NF-κB path-way. *3 Biotech*, 2021, 11(6): 258-263. [Crossref]

58. Hong W, Xu XY, Qiu ZH, Gao JJ, Wei ZY, Zhen L, *et al*. Sirt1 is involved in decreased bone formation in aged apolipoprotein E-deficient mice. *Acta Pharmacol Sin*, 2015, 36(12): 1487-1496. [Crossref]

59. Zhu C, Ding H, Shi L, Zhang S, Tong X, Huang M, *et al*. Exercise improved bone health in aging mice: a role of SIRT1 in regulating autophagy and osteogenic differentiation of BMSCs. *Front Endocrinol (Lausanne)*, 2023, 14: 1156637. [Crossref]

60. Kou Y, Rong X, Tang R, Zhang Y, Yang P, Liu H, *et al*. Eldecalcitol prevented OVX-induced osteoporosis through inhibiting BMSCs senescence by regulating the SIRT1-Nrf2 signal. *Front Pharmacol*, 2023, 14: 1067085. [Crossref]

61. Li Y, Sun W, Li J, Du R, Xing W, Yuan X, *et al*. HuR-mediat-

ed nucleocytoplasmic translocation of HOTAIR relieves its inhibition of osteogenic differentiation and promotes bone formation. *Bone Res*, 2023, 11(1): 53-69. [Crossref]

62. Arai M, Ochi H, Sunamura S, Ito N, Nangaku M, Takeda S, *et al*. A Novel Long Noncoding RNA in Osteocytes Regulates Bone Formation through the Wnt/β-Catenin Signaling Pathway. *Int J Mol Sci*, 2023, 24(17): 13633. [Crossref]

63. Freitas J, Moura S, Barbosa M, Santos SG, & Almeida. Long non-coding RNA CASC2 regulates osteoblasts matrix mineralization. *Front Bioeng Biotechnol*, 2023, 11: 1155596. [Crossref]

64. Lin S, Wen Z, Li S, Chen Z, Li C, Ouyang Z, *et al*. LncRNA NEAT1 promotes the macrophage inflammatory response and acts as a therapeutic target in titanium particle-induced osteolysis. *Acta Biomater*, 2022, 142: 345-360. [Crossref]

65. Fan Y, Wang L, Han X, Ma H, Zhang N, & She L. LncRNA ASB16-AS1 accelerates cellular process and chemoresistance of ovarian cancer cells by regulating GOLM1 expression via targeting miR-3918. *Biochem Biophys Res Commun*, 2023, 675: 1-9. [Crossref]

66. Wang YW, Zhu WJ, Ma RR, Tian YR, Chen X, & Gao P. PIN1P1 is activated by CREB1 and promotes gastric cancer progression via interacting with YBX1 and upregulating PIN1. *J Cell Mol Med*, 2023, 00: 1-11. [Crossref]

67. Tang Y, Ma N, Luo H, Chen S, &Yu F. Downregulated long non-coding RNA LINC01093 in liver fibrosis promotes hepatocyte apoptosis via increasing ubiquitination of SIRT1. *J Biochem*, 2020, 167(5): 525-534. [Crossref]
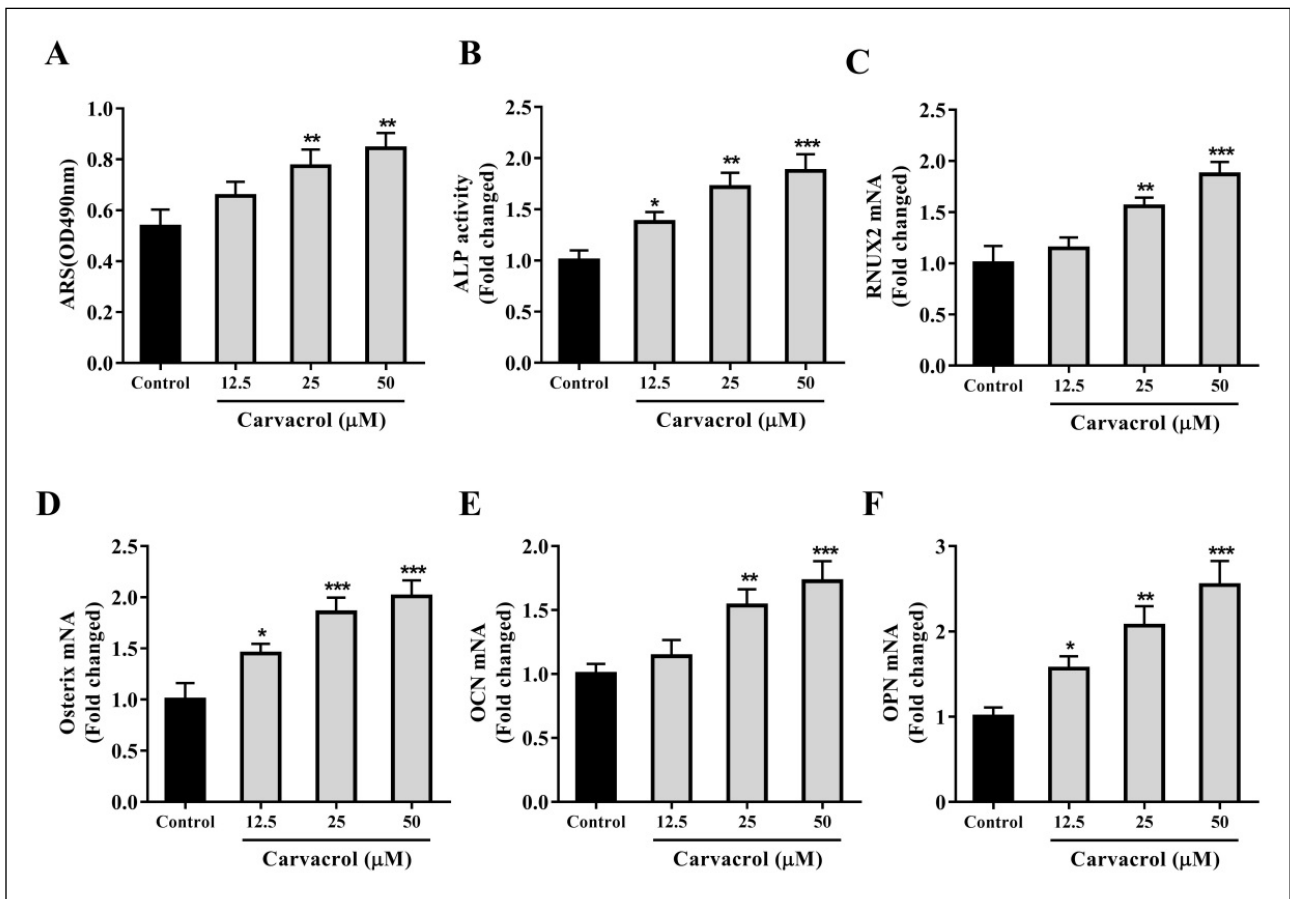
Figure S1. Determination of the concentration of carvacrol to promote the differentiation of BMSCs into osteoblasts. BMSCs were pretreated with different concentrations of carvacrol (12.5, 25, and 50 μM). (**A**) Detection of ALP activity. (**B**) Ratio of the area of purple calcium phosphate nodules to the total area after staining. (**C**-**F**) BMSCs were harvested after treatment with carvacrol for 7 days, and the expression levels of RUNX2, Osterix, OCN, and OPN were measured by RT-qPCR. Data are presented as mean ± SD. One-way ANOVA was performed by Tukey's multiple comparison test. *$P < 0.05$, **$P < 0.01$, ***$P < 0.001$ *vs*. the control group.